High-resolution x-ray diffraction analysis of epitaxially grown indium phosphide nanowires

T. Kawamura,[a] S. Bhunia,[b] and Y. Watanabe[c]
Basic Research Laboratories, Nippon Telegraph and Telephone Corporation, 3-1, Wakamiya, Morinosato, Atsugi 243-0198, Japan

S. Fujikawa, J. Matsui,[d] Y. Kagoshima, and Y. Tsusaka
University of Hyogo, 3-2-1, Kamigori, Ako 678-1297, Japan

(Received 27 July 2004; accepted 10 January 2005; published online 11 April 2005)

Indium phosphide (InP) nanowires epitaxially grown on InP (111)B were investigated by using grazing incidence x-ray diffraction. A broad scattering at the tail of InP $(2\bar{2}0)$ diffraction and an additional peak at the low angle side were observed, showing the formation of nanowires and alloys of the gold catalysts and indium. Scattering intensity along the $[1\bar{1}0]$ direction was compared with calculations based on a cylinder model. The best fit was obtained for a 5.5-nm radius with a 2.5-nm deviation, which was smaller than the values determined from the secondary electron microscopy and photoluminescence spectroscopy measurements. This result is explained by an oxide layer on the nanowire sidewalls and the low quantum efficiency of photoluminescence yields for small nanowires since x-ray diffraction directly detects crystalline structure of nanowires. © *2005 American Institute of Physics*. [DOI: 10.1063/1.1863418]

I. INTRODUCTION

Quasi-one-dimensional semiconductor structures are attracting much attention because of their diversity for future electronic and photonic device applications.[1] For nanostructures below ten nanometers, quantum effects mainly determine the electrical and optical properties, giving rise to significant changes in electron transportation and optical luminescence, which are very important for quantum computing and quantum communications.

Ever since the fabrication of Si submicron whiskers by means of the vapor-liquid-solid (VLS) mechanism,[2] a number of nanowires, including Si, GaAs, InAs, and InP, have been grown using the chemical-vapor deposition, chemical beam epitaxy, and laser-assisted catalytic growth. Critical issues in the nanowire growth are the control and characterization of nanowire size because nanowire size and its distribution govern the macroscopic electrical properties. Scanning electron microscopy (SEM) and transmission electron microscopy (TEM) have been used to determine the nanowire size and its distributions in spite of the limitation of applicable area. However, the relationship between the macroscopic properties and nanowire dimensions is still uncertain because of the lack of an evaluation technique.

Owing to the high sensitivity of Bragg profiles for determining the size and shape of crystals,[3] small structures, such as quantum dots and nanowires, can be evaluated by analyzing x-ray scattering profiles. Recently, quantum dot structures on a surface and in buried layers have been analyzed by observing scattering profiles at Bragg diffraction.[4] This technique has also been applied to evaluate artificial structures on a substrate[5] and has showed local strain and defects in the structures. The x-ray diffraction technique has also been applied for the characterization of nanowire structures and has shown the order of alignment, degree of crystallization, and nanowire quality.[6] However, due to the low angle resolution and lower degree of alignment of nanowires, precise evaluations of nanowires have not yet been performed. In this paper, we present the results of x-ray scattering measurement of epitaxially grown nanowires and an analysis of nanowire size and its distribution using a cylinder model.

II. EXPERIMENT

InP nanowires were grown on InP (111)B substrate using a low-pressure metal-organic vapor-phase epitaxy (MOVPE) system with tertiarybutyl phosphine (TBP) and trimethylindium (TMI) as precursors. Gold colloidal particles about 20 nm in diameter were first spread on the substrate as catalysts. At the beginning of the growth procedure, the substrate was annealed at 500 °C for cleaning and desorbing the extraorganics of gold catalysts. It was then cooled to 450 °C and InP nanowires were formed under several growth conditions. Prior to x-ray measurement, nanowire size was evaluated by TEM, high-resolution SEM, and photoluminescence spectroscopy (PL). The detailed growth procedure and the results of SEM, TEM, and PL measurements are described in Ref. 9.

X-ray measurement was performed at beamline 24XU of the SPring8 synchrotron facility. The substrate was set on the z-axis goniometer,[7] and the x-ray intensity was measured at $(2\bar{2}0)$ Bragg diffraction with a position sensitive detector. Incident x-rays of 0.124-nm wavelength were collimated to 150 μm $\times$ 1 mm for the vertical and horizontal directions,

[a]Electronic mail: kawamura@will.brl.ntt.co.jp
[b]Present address: Saha Institute of Nuclear Physics, Kolkata, India.
[c]Present address: NTT Advanced Technology Co., Atsugi, Japan.
[d]Present address: Center of Advanced Science and Technology Ako, Japan.

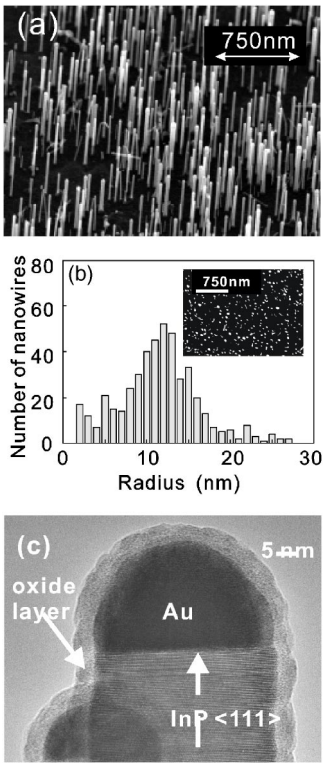

FIG. 1. (a) SEM image of InP nanowires. (b) The size distribution of nanowire radii estimated from the size of gold catalysts. Inset shows the plan view of nanowires with gold particles. (c) TEM image of nanowires. The inset arrow indicates the oxide layer formed on the InP nanowires.

and impinged upon the substrate at 0.2° incident angle. To reduce scattering from the substrate, a solar slit with 0.2° divergence was set in front of the detector.

III. RESULTS AND DISCUSSION

A. SEM and PL observations

Figure 1(a) shows a field-emission SEM image of nanowires with a 40° tilting angle with respect to the surface normal. Free-standing nanowires with uniform heights were observed, suggesting that the growth proceeded via the VLS mechanism. The variation in diameter was evaluated from the distribution of the size of gold particles on the top of the nanowires. Figure 1(b) shows the histogram of a gold particle size, and inset is a SEM image of nanowires viewed from the top without tilting. Although the size distribution in the SEM images seems small, nanowire radius in the histogram varies between 2 and 20 nm with the mean value of 13 nm and the deviation of 3 nm, showing that the gold particles coalesced during the annealing and growth processes. Figure 1(c) is a typical high-resolution TEM image of a thick nanowire and the gold catalyst particle. Both the image of the InP nanowires and oxide layer (arrow) were clearly observed. The estimated oxide layer thickness is about 5 nm, which is thicker than the usual native oxide and contamination layers, and the oxide layers covered the nanowires and gold particles, suggesting that these layers were formed after the nanowire growth.

Figure 2 shows the PL spectra of nanowires and InP (111)B without nanowires at room temperature. A clear peak

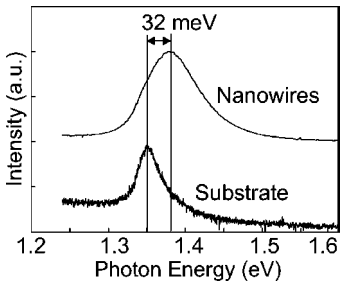

FIG. 2. PL spectra of nanowires and InP (111)B substrate. A 32-meV energy shift was clearly observed, suggesting the quantum confinement in nanowires.

shift of 32 meV was observed, showing the quantum confinement of the nanowires. The diameter of the nanowires was obtained from the peak-shift value and calculations based on the cylinder model[8] and was about 18 nm.[9] By considering the TEM observations,[9] the difference of the nanowire size of SEM and PL could be explained by the existence of the oxide layer on the sidewall of nanowires.

B. GIXD measurement

Figure 3 shows the x-ray profiles of ω and θ–2θ scans. The scan direction in reciprocal space is shown in the inset. Both profiles show a sharp bulk peak and broad scattering from the nanowires at the tail of the Bragg diffraction. The peak width of the nanowires in the ω scan is more than six times as large as that in the θ–2θ scan, suggesting a small variation of the d-spacing value and large deviation from the growth direction. From the analysis of the ω-scan profile, the divergence was estimated to be 0.42° along the [111] direction. Additionally, the peak position of the nanowires was 0.07° larger than that of bulk diffraction, suggesting that the nanowires have compressive stresses along the $[\bar{2}20]$ direction.

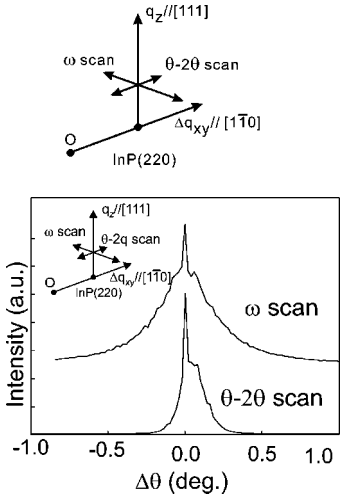

FIG. 3. Bragg profiles of $(\bar{2}20)$ for the ω scan and θ-2θ scan. Inset shows the scan direction in reciprocal space for each measurement. Both profiles show a sharp bulk peak and broad scattering from nanowries. The peak broadening of the ω-scan profile is explained by the angle deviation of nanowires. In the θ-2θ scan profile, a peak shift of nanowire scattering is observed, suggesting shrinking of the d-spacing of nanowires.

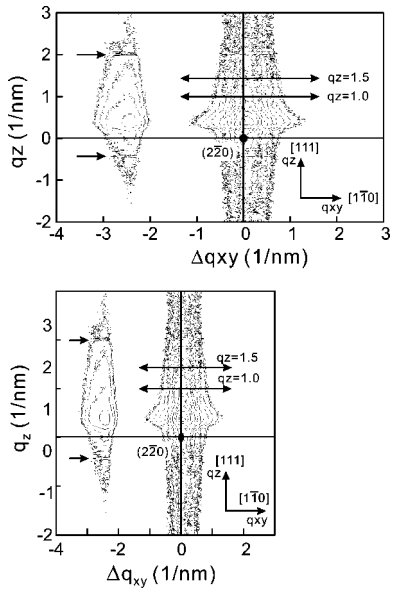

FIG. 4. Intensity distribution at InP $(2\bar{2}0)$. The origin of q_z and $\Delta q_{xy}[=q_{xy}-q_{xy}(2\bar{2}0)]$ was set at the exact position of $(2\bar{2}0)$ diffraction. The observed Bragg position shifted to $q_z>0$ region due to the total reflection effect.

Figure 4 shows the intensity distribution at InP $(2\bar{2}0)$ in the logarithmic scale.[10] The origin and direction of $\Delta q_{xy}[=q_{xy}-q_{xy}(2\bar{2}0)]$ and q_z are also shown.

Two regions of x-ray scattering at $\Delta q_{xy}=0.0$ and -2.5 nm^{-1} were observed, suggesting the formation of nanowires and additional single crystals related to nanowire growth. The possible origins of this extra scattering are gold–InP alloys, such as Au_3In (002), Au_7In_3 (402), and Au_2P_3 (−112), whose *d*-spacing values in the ICDD database were similar to the peak at $\Delta q_{xy}=-2.5$ nm^{-1}. It should be noted that the crystal structure of gold alloys could not be established because x-ray diffractions from other Bragg indices were not measured. The streaks along Δq_{xy} at $q_z=-0.5$ and 2.0 nm^{-1} are artifacts of the position sensitive detector.

Since the x-ray scattering profile depends on nanowire shape and size, macroscopic structural properties of nanowires, such as the average radius and its distribution, can be obtained by analyzing the scattering profile. The distribution of the nanowire size in Fig. 1(b) shows asymmetry with a large tail at larger particle sizes, and standard distribution function is not appropriate. Several functions can describe such distribution,[11] and here we selected the γ-distribution function, which has also been used for analyzing x-ray scattering data of porous materials.[12] The distribution functions used in the data analysis are as follows:

$$G[t(r,R_o),N]=\frac{t^{N-1}e^{-t/2}}{2^N\Gamma(N)}. \tag{1}$$

$$t(r,R_o)=2(N-1)\frac{r}{R_o}. \tag{2}$$

$$\sigma_g=\frac{\sqrt{N}}{N-1}R_o. \tag{3}$$

Here $G[t(r,R_o),N]$ and σ_g are the normalized γ-distribution function and its dispersion, respectively. N is the freedom parameter, describing the dispersion, and R_o is the mean value of nanowires.

Another feature we should consider for the analysis of x-ray scattering is the nanowire shape. When the nanowire size was small and some tens of nanometers and only the number of unit cells is included, x-ray diffraction from the nanowire cannot be treated as a δ-function even in the ideal case. The size and shape effects in x-ray scattering for small crystals have been investigated for many kinds of shapes, and first-order Bessel function can be used for cylindrical shapes.[3,13]

Finally, we obtained the x-ray scattering function with the parameters of the nanowire size and its distribution, shape, and momentum-transfer vector $q=(\Delta q_{xy},q_z)$, as follows:

$$I(\Delta q_{xy},q_z)=I^B(\Delta q_{xy},q_z)+I^{\mathrm{NW}}(\Delta q_{xy},q_z). \tag{4}$$

$$I^{\mathrm{NW}}(\Delta q_{xy},q_z)=\mathrm{const.}|F(q_{xy},q_z)|^2 \times\frac{\sin(2\pi q_zH)}{2\pi q_zH}\int_0^\infty|S_{\mathrm{cyl}}(\Delta q_{xy})|^2G[t(r,R_o),N]dr. \tag{5}$$

$$S_{\mathrm{cyl}}(\Delta q_{xy})=2\pi r^2\frac{J_1(\Delta q_{xy}r)}{\Delta q_{xy}r}. \tag{6}$$

Here I^B and I^{NW} are the intensity from the substrate and nanowires, and $F(q_{xy},q_z)$ and $S_{\mathrm{cyl}}(\Delta q_{xy})$ are the structure factor of InP crystal and form factor of cylinder shape, respectively. The structure of nanowires is described by the height H, radius R_o, and freedom parameter N, which is related to the dispersion of nanowire radius [Eq. (3)]. The form of the distribution function $G[t(r,R_o),N]$ was already described in Eq. (1).

Since terms related to q_z and Δq_{xy} have no correlation, one can analyze the intensity distribution along q_z and Δq_{xy} independently. Considering that the intensity of thermal diffuse scattering is stronger at the Bragg diffraction of InP (220), scattering profiles at $q_z=1.0$ and 1.5 nm^{-1} were chosen for the analysis. During the fitting procedure, nanowire radius and its dispersion, the intensity ratio between bulk crystal truncation rod (CTR) scattering, and nanowire scattering were optimized to minimize the errors between the measured and calculated Bragg and scattering profiles in the linear scale and profiles in the tail region were not optimized intentionally.

After a number of calculations, the best fit was obtained with $R=5.0$ nm and $N=5$, which corresponds to a 2.5-nm deviation of nanowire radius. Calculated and measured profiles at $q_z=1.0$ and 1.5 nm^{-1} are shown in Figs. 5(a) and 5(b), where the calculations used parameters obtained from SEM and PL observations. Obviously, good agreement was obtained with the parameters of x-ray measurement, although

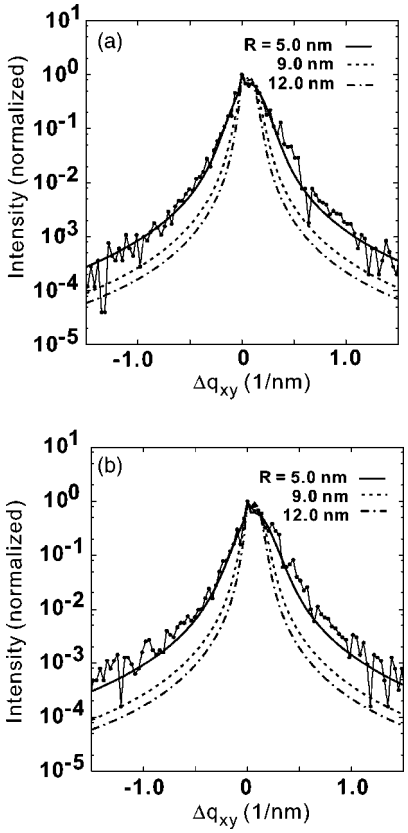

FIG. 5. Measured and calculated profiles at (a) $q_z=1.0$ and (b) 1.5 nm^{-1}. Average size and its dispersion were optimized with $q_z=1.0$ nm^{-1}, and the scattering profile at 1.5 nm^{-1} was calculated using these values. Profiles using size and its dispersion determined from SEM and PL measurement show smaller peak widths, suggesting low sensitivity for smaller nanowires.

the profiles of SEM and PL parameters show large differences. It should be noted that the empirical x-ray scattering profiles, such as Lorentz and Voigt functions, also showed large differences at the tail of the scattering profiles, indicating that the shape and size distribution of nanowires has severe effects on the scattering profiles.

Figure 6 shows the relations between the nanowire size and the confinement energy of InP nanowires with an infinite barrier. The energy determined from x-ray scattering measurement and SEM observation differ from that of PL measurement, and the difference of x-ray and PL measurements

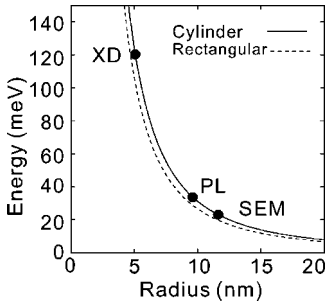

FIG. 6. The confinement energy of InP nanowires with an infinite barrier. The solid and dashed lines correspond to the cylindrical and rectangular shape, respectively. The energy determined from PL measurement is larger than that from x-ray measurement, suggesting that the quantum efficiency of small nanowires is lower.

is larger than SEM observation. Considering that there are some oxide layers with thickness of some nanometers on the sidewall of nanowires,[9] the mean value estimated from SEM observations should become larger than the real ones. Additionally, defocusing errors in this range cannot be neglected, and they also would increase the observed mean value of nanowire radius.

However, the large difference between the x-ray measurement and PL technique cannot be understood by only the existence of the oxide layers. One possible reason for the difference is the volume effect in PL measurement. Since the nanowire size dependence of quantum efficiency is not known, we supposed that the PL intensity from each wire was the same. If the PL intensity from large nanowires is stronger than that from small ones, the real mean size of nanowires becomes smaller than that estimated from the peak-shift value. In this case, the decrease of the mean size depends on the dispersion of distribution, and it is about 70% for γ-distribution function with a freedom parameter of $N=5$.

Another possible reason is the different sensitivity of the two techniques. Any nanowire that maintains crystal structure can be detected by x-ray scattering, whereas the PL technique only detects luminescent nanowires. When the luminescence from smaller nanowires is weaker than that from larger ones, the mean value of nanowires increases, and this would also explain the difference of the mean value between the x-ray and PL measurements.

IV. CONCLUSION

In conclusion, we investigated the structural properties of InP nanowires grown on InP (111)B using SEM, PL, and high-resolution x-ray diffraction. SEM and PL observations showed that nanowires with uniform heights were formed via the VLS mechanism, and wire size was similar to that of catalyst particles. From the analysis of in-plane Bragg diffraction, shrinking of nanowires along $[1\bar{1}0]$ direction and 0.4° dispersion of nanowire direction along [111] were observed. The nanowire size and its dispersion were evaluated from the scattering profile, and a 5-nm radius and a 2.5-nm dispersion were obtained. This radius was smaller than that determined from SEM and PL observation. The possible reason is that the x-ray scattering technique detects crystalline parts of wires, while SEM and PL techniques should consider additional factors, such as oxide layers on the nanowires and different quantum efficiencies in nanowires of different size.

[1]X. Duan, Y. Huang, Y. Cui, J. Wang, and C. M. Lieber, Nature (London) **409**, 66 (2001).
[2]R. S. Wagner and W. C. Ellis, Appl. Phys. Lett. **4**, 89A (1964).
[3]A. L. Patterson, Phys. Rev. **56**, 972 (1939).
[4]M. Gailhanou, T. Baumbach, U. Marti, P. C. Silva, F. K. Reinhart, and M. Ilegems, Appl. Phys. Lett. **62**, 1623 (1993).
[5]V. Holý, A. A. Darhuber, and G. Bauer, Phys. Rev. B **52**, 8348 (1995).
[6]M. H. Huang, Y. Wu, H. Feick, N. Tran, E. Weber, and P. Yang, Adv. Mater. (Weinheim, Ger.) **13**, 113 (2001).
[7]T. Kawamura, Y. Watanabe, Y. Utsumi, K. Uwai, J. Matsui, Y. Kagoshima, Y. Tsusaka, and S. Fujikawa, J. Cryst. Growth **221**, 106 (2000).
[8]For example, L. I. Schiff (McGraw-Hill, New York,).

[9]S. Bhunia, T. Kawamura, Y. Watanabe, S. Fujikawa, and K. Tokushima, Appl. Phys. Lett. **83**, 3371 (2003).
[10]q_{xy} and q_z are the compositions of the scattering vector along in-plane and normal to the surface, respectively.
[11]M. Zinke-Allmang, L. C. Feldman, and M. H. Grrabow, Surf. Sci. Rep. **16**, 377 (1992).
[12]K. Omote, Y. Ito, and S. Kawamura, Appl. Phys. Lett. **82**, 544 (2003).
[13]M. von Laue, Ann. Phys. **26**, 55 (1936).